Theoretical Investigation of Ion Pair S_N2 Reactions of Alkali Isothiocyanates with Alkyl Halides. Part 1. Reaction of Lithium Isothiocyanate and Methyl Fluoride with Inversion Mechanism

HUA-JIE ZHU,[1] YI REN,[2] JIE REN,[1] SAN-YAN CHU[3]
[1]*State Key Lab of Phytochemistry and Plant Resources in West China, CAS, Kunming, P.R.China*
[2]*College of Chemistry, Sichuan University, Chengdu 610064, P.R.China*
[3]*Department of Chemistry, National Tsing Hua University, Hsinchu, Taiwan*

Received 7 January 2004; accepted 22 April 2004

DOI 10.1002/qua.20213

ABSTRACT: The gas-phase ionic S_N2 reactions NCS^- + CH_3F and ion pair S_N2 reaction LiNCS + CH_3F with inversion mechanism were investigated at the level of MP2(full)/6-311+G**//HF/6-311+G**. Both of them involve the reactants complex, inversion transition state, and products complex. There are two possible reaction pathways in the ionic S_N2 reaction but four reaction pathways in the ion pair S_N2 reaction. Our results indicate that the introduction of lithium significantly lower the reaction barrier and make the ion pair displacement reaction more facile. For both ionic and ion pair reaction, methyl thiocyanate is predicted to be the major product, but the latter is more selective. More-stable methyl isothiocyanate can be prepared by thermal rearrangement of methyl thiocyanate. The theoretical predictions are consistent with the known experimental results. © 2004 Wiley Periodicals, Inc. Int J Quantum Chem 101: 104–112, 2005

Key words: ab initio; inversion mechanism; isothiocyanate; reaction pathway; S_N2; thiocyanate

Correspondence to: Y. Ren; e-mail: yiren57@hotmail.com

Contract grant sponsors: CAS; State Education Ministry; Sichuan University; NSC of Taiwan

Introduction

Isothiocyanates are very reactive molecules [1] but less so than isocyanates. Some are physiologically active and occur as natural products. For example, allyl isothiocyanate $CH_2{=}CHCH_2NCS$ is a major component of mustard oil and horseradish root. Isothiocyanates can be prepared by thermal rearrangement of the analogous thiocyanates isomer, which can be obtained by treatment of alkyl halides or tosylates with alkali metal thiocyanate [2] (Eq.1). This is a practical route for the synthesis of organic thiocyanate and isothiocyanate.

$$\mathrm{MNCS} + \mathrm{RX} \rightarrow \mathrm{RSCN} \rightarrow \mathrm{RNCS}. \qquad (1)$$

Unlike the anionic S_N2 reactions, the ion pair S_N2 reactions have been less studied theoretically, although some experiment results are known [3–8]. Harder et al. [9] studied some identity ion pair S_N2 reactions at carbon $MX + CH_3X$ (M = Li, Na; X = F, Cl) at the level of MP4/6-31+G*//HF/6-31+G*. Streitwieser et al. [10] extended the work to the higher alkyls with restricted Hartree–Fock (RHF), second-order Møller–Plesset (MP2), and Becke's three-parameter exchange functional and the gradient-corrected functional of Lee, Yang, and Paar (B3LYP) methods with 6-31+G* and discussed some steric effects for the ion pair displacement reactions. Leung and Streitwieser [11] investigated the structures of lithium and sodium cyanates and their related monomeric ion pair, and dimeric ion pair S_N2 reactions with methyl halides, $Y + CH_3X$ [Y = MNCO, MOCN, $(MNCO)_2$ (M=Li and Na); X =F, Cl]. Their calculated results show that methyl cyanate should form preferentially via a six-membered ring transition-state (TS) structure on analyses of transition structures if the reaction involves a monomer ion pair inversion pathway. More recently, Ren and Chu [12] reported the higher G2M(+) level calculations for the identity ion pair S_N2 reactions at nitrogen $LiX + NH_2X$ (X = F, Cl, Br and I) and at carbon $LiX + CH_3X$ (X = F, Cl, Br and I) [13]. These results indicate that the ion pair S_N2 reactions involve preliminary encounter dipole–dipole complex instead of a negatively charged ion–dipole complex in anionic S_N2 reaction, then proceeds via a cyclic transition structure.

To the best knowledge of the current authors, as the analogous reactions of alkali metal cyanates and isocyanates with alkyl halides, ion pair S_N2 reactions of alkali metal isothiocyanates with alkyl halides have not previously been investigated theoretically. Theoretical investigation should shed light on the details of molecular mechanism of the organic reactions. In this article, we present a comprehensive theoretical study on the monomer ion pair S_N2 reaction of lithium thiocyanate and methyl fluoride [Eq. (2)] with inversion mechanism. All possible reactants and products complexes and six-membered and four-membered ring (TS) structures were considered. One aim of this article is to address some similarities and differences between the ion pair S_N2 reactions of thiocyanates and cyanates. We hope these studies obtained by ab initio molecular orbital (MO) calculations can explain the experimental results in a reasonable manner and promote further understanding of the mechanism of the ion pair S_N2 reaction at carbon. To compare the anionic and ion pair reaction, the energetics for the reaction [Eq. (3)] was also calculated at the same level.

$$\mathrm{LiNCS} + \mathrm{CH_3F} \rightarrow \mathrm{CH_3SCN} + \mathrm{LiF} \qquad (2)$$

$$\mathrm{NCS^-} + \mathrm{CH_3F} \rightarrow \mathrm{CH_3SCN} + \mathrm{F^-}. \qquad (3)$$

Methodology

Veszprémi et al. [14] pointed out that the correlation energy should be included if a good description of the bonding was required in the structures of some pseudohalides, -NCO, -NCS, and $-N_3$. In this work, the geometries of all species were fully optimized using HF/6-311+G**. The electron correlation effect was taken into account by further single-point MP2 [15] calculation, with all electrons being included in the correlation treatments, that is, MP2(full)/6-311+G**//HF/6-311+G**, hereafter designated MP2(full). All stationary points were characterized using frequency analysis at HF/6-311+G** level, and scaled vibrational zero-point energies (ZVPE) by a factor of 0.9248 [16] were included in the calculations of relative MP2(full) energies. Charge distributions were obtained from the wavefunctions calculated at the MP2(full) /6-311+G** level on the HF geometries, employing natural population analysis (NPA) [17]. All calculations were performed using Gaussian 98 system of program [18].

Throughout this paper, all internuclear distances are in angstrom (Å), and bond angles are in degree (°). Relative energies in kJ/mol within the text cor-

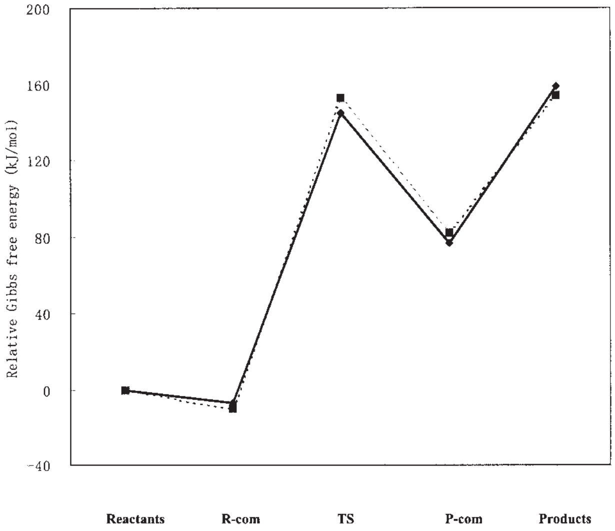

SCHEME 1. Schematic potential energy profile for the gas-phase displacement reaction NCS^- + CH_3F. Solid line represents the reaction SCN^- + $CH_3F \rightarrow CH_3NCS + F^-$ and dashed line represents the reaction NCS^- + $CH_3F \rightarrow CH_3SCN + F^-$. All Gibbs free energies are given relative to reactants.

respond to the enthalpy changes (ΔH_{298}) and the Gibbs free energy changes (ΔG_{298}) at 1 atm and 298.15 K.

Results and Discussion

The potential energy surface for the gas-phase reactions between methyl fluoride with thiocyanate ion and lithium isothiocyanate, respectively, can be described by an unsymmetrical double-well potential curve corresponding to the nonidentity S_N2 reaction (see Scheme 1 and Scheme 2). The substitution reaction involves the initial formation of a reactants ion–dipole or dipole–dipole complex (R-com), releasing the complexation energy. This R-com must then overcome the activation barrier to reach an inversion (TS) structure. The latter then breaks down to give the product's ion–dipole or dipole–dipole complex (P-com), which subsequently dissociates into the separate products. Calculated total and the relative energies of all stationary points involved in reactions 2 and 3 are listed in Table I and II, respectively.

REACTANTS AND PRODUCTS

The predicted main geometries of thiocyanate anion and lithium isothiocyanate are listed in Figures 1 and 2. Previous studies of Veszprémi et al. [14] indicated that there were three possible isomers formed by lithium and –NCS. Linear lithium isothiocyanate (**2b**′) and T-shape structure (**2a**′) are stable on the potential energy surface, but the linear thiocyanate does not exist. The T-shape isomer (**2a**′), in which a π-complex is achieved between the empty orbital of lithium and the π-system of thiocyanate (-NCS) group, is more stable. Our results show that **2a**′ is lower than **2b**′ by 3.4 kJ/mol in terms of ΔH_{298}. The equilibrium isomerization barrier is ca.17 kJ/mol at the level of MP2(full).

Calculated geometrical parameters of two main products—methyl thiocyanate (**6a**) and methyl isothiocyanate (**6b**)—are shown in Figure 2. At the HF/6-311+G** level, **6a** has a bent structure at the sulfur atom and **6b** has a linear structure. Product **6b** was found to be 4.4 kJ/mol (in terms of ΔH_{298}) more stable than **6a**, similar to the isomerization of allyl thiocyanate to allyl isothiocyanate, where isothiocyanate is lower in energy than allyl thiocyanate by >13 kJ/mol [19].

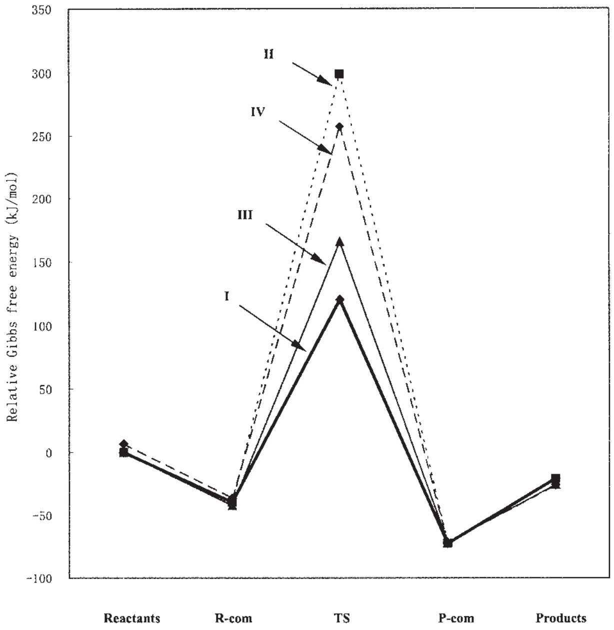

SCHEME 2. Schematic potential energy profile for the gas-phase displacement reaction LiNCS + CH_3F with inversion mechanism. Numerals **I**, **II**, **III,** and **IV** represent the four possible reaction pathways. All Gibbs free energies are given relative to reactants.

TABLE I

Calculated total energies (hartree) for species involved in the exchange reactions of NCS^- + CH_3F and LiNCS + CH_3F.

	HF/6-311+G**		MP2(full)/6-311+G**//HF/6-311+G**	
	H (298K)	G (298K)	H (298K)	G (298K)
CH_3F (**1**)	−139.040895	−139.006106	−139.451664	−139.476875
NCS^- (**2**)	−489.916876	−489.943230	−490.505421	−490.531775
$NCS^- \cdots CH_3F$ (**3a**)	−628.966609	−629.009749	−629.968042	−630.011182
$SCN^- \cdots CH_3F$ (**3b**)	−628.967292	−629.011529	−629.968179	−630.012416
$[NCS \cdots CH_3 \cdots F]^{-\neq}$ (**4a**)	−628.894547	−628.933360	−629.914772	−629.953585
$[SCN \cdots CH_3 \cdots F]^{-\neq}$ (**4b**)	−628.898711	−628.937298	−629.912044	−629.950631
$NCSCH_3 \cdots F^-$ (**5a**)	−628.913287	−628.952831	−629.940003	−629.979547
$SCNCH_3 \cdots F^-$ (**5b**)	−628.916882	−628.955917	−629.938428	−629.977463
CH_3SCN (**6a**)	−529.430691	−529.464132	−530.195139	−530.228580
CH_3NCS (**6b**)	−529.435414	−529.468991	−530.196872	−530.230449
F^- (**6c**)	−99.460084	−99.459907	−99.703232	−99.719751
LiNCS (cyc.) (**2a′**)	−497.361982	−497.393569	−497.975113	−498.006700
LiNCS (line.) (**2b′**)	−497.367383	−497.397683	−497.973813	−498.004113
R-com1 (**3a′**)	−636.426753	−636.473508	−637.451855	−637.498610
R-com2 (**3b′**)	−636.429110	−636.473551	−637.455227	−637.499668
R-com3 (**3c′**)	−636.434497	−636.479446	−637.452448	−637.497397
TS1 (**4a′**)	−636.366321	−636.405119	−637.398807	−637.437605
TS2 (**4c′**)	−636.316619	−636.356257	−637.330045	−637.369683
TS3 (**4b′**)	−636.351086	−636.390642	−637.380885	−637.420441
TS4 (**4d′**)	−636.330135	−636.371860	−637.343809	−637.385534
P-COM1 (**5a′**)	636.549062	636.507536	−637.469620	−637.511146
P-COM2 (**5b′**)	−636.432897	−636.474410	−637.469318	−637.510831
LiF (**6c′**)	−106.969977	−106.992715	−107.240119	−107.262857

TABLE II

The relative enthalpies (kJ/mol), ΔH_{298}[a], and Gibbs free energies (kJ/mol), ΔG_{298}[b], with respect to the reactants at 298.15K for the anionic S_N2 reaction NCS^- + CH_3F and the ion pair S_N2 reaction LiNCS + CH_3F.

Pathway	Reactants	R-com	TS	P-com	Products	Products
NCS^- + CH_3F	0.0	−28.8[a]	111.1	44.8	154.2	CH_3SCN + F^-
	0.0	**−6.6**[b]	**144.6**	**76.4**	**158.4**	
SCN^- + CH_3F	0.0	−29.1	118.3	49.0	149.6	CH_3NCS + F^-
	0.0	**−9.9**	**152.3**	**81.9**	**153.5**	
I	0.0	−65.8	73.4	−112.5	−22.3	CH_3SCN + LiF
	0.0	**−39.5**	**120.7**	**−72.4**	**−20.6**	
II	0.0	−65.8	254.0	−112.5	−22.3	CH_3SCN + LiF
	0.0	**−39.5**	**299.0**	**−72.4**	**−20.6**	
III	0.0	−74.7	120.5	−111.7	−26.8	CH_3NCS + LiF
	0.0	**−42.3**	**165.8**	**−71.6**	**−25.5**	
IV	0.0	−70.8	214.4	−115.1	−30.2	CH_3NCS + LiF
	0.0	**−43.1**	**250.6**	**−78.4**	**−32.3**	

[a] Relative enthalpies in regular font.

[b] Relative free Gibbs energies in bold.

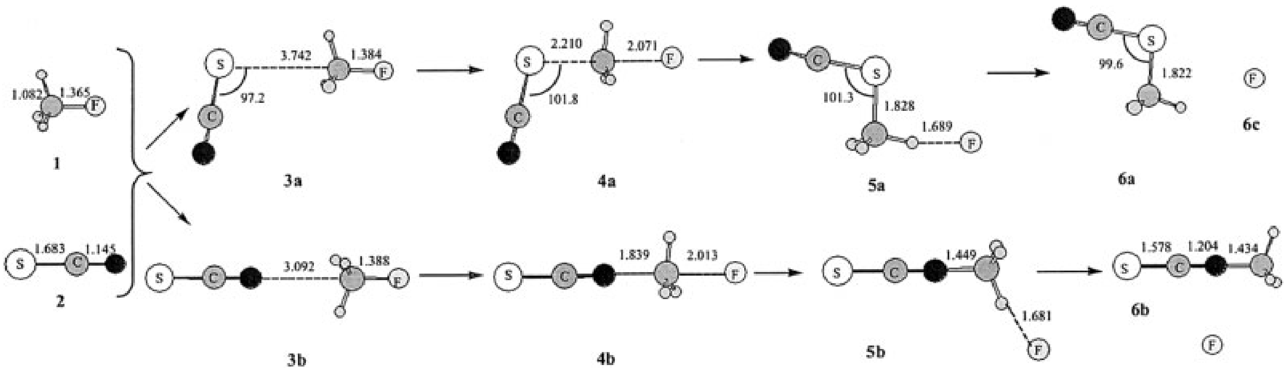

FIGURE 1. Main geometries of the reactants, reactants and products ion–dipole complexes, transition structures, and products for the reaction $NCS^- + CH_3F$ at the level of HF/6-311+G(d, p).

REACTANTS AND PRODUCTS COMPLEXES

In the reaction NCS^-+CH_3F, two reactants ion–dipole complexes are found. Through coordinating with three hydrogen atoms to form R-com, $NCS^- \cdots CH_3F$ (**3a**) or $SCN^- \cdots CH_3F$ (**3b**), SCN^- can approach CH_3F. The shorter N–H distances and more electronegativity of nucleophilic site (N) make **3b** a little bit lower in complexation energy than **3a** by 3.3 kJ/mol, in terms of ΔG_{298}. The other two products ion–dipole complexes involved in the anionic S_N2 reaction are $F^- \cdots CH_3SCN$ (**5a**) and $F^- \cdots CH_3NCS$ (**5b**), in which the fluoride ion coordinates with only one hydrogen atom.

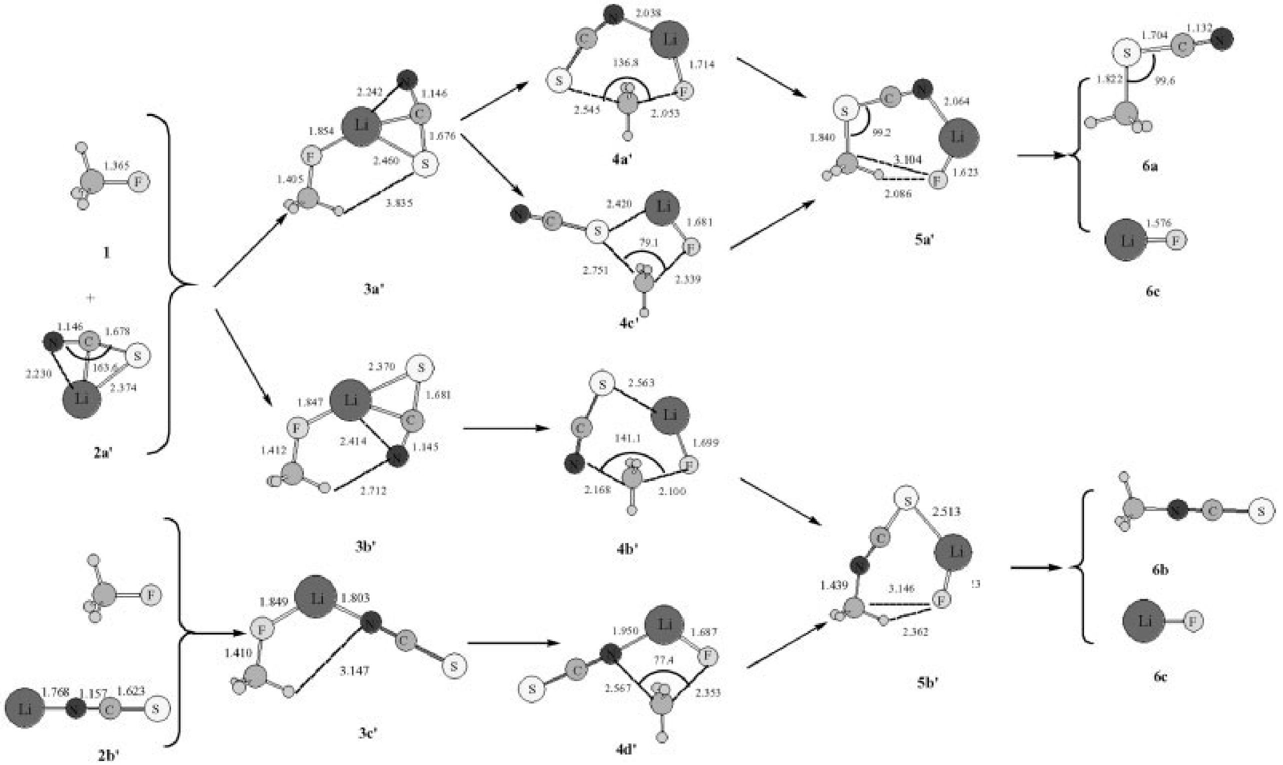

FIGURE 2. Main geometries of the reactants, reactants and products dipole–dipole complexes, transition structures, and products for the reaction $LiNCS + CH_3F$ at the level of HF/6-311+G(d, p).

There are three possible stable conformers for the reactants dipole–dipole complexes, **3a′–c′**, formed by methyl fluoride and lithium isothiocyanate. All of these conformers place the lithium cation in complexing with the halogen to form a so-called "X-philic" reactants complex $CH_3F \cdots LiNCS$. Lithium isothiocyanate keeps T-shape structure in **3′–b′** but linear structure in **3c′**. In forming **3a′**, the incoming lithium cation strongly interacts with fluorine atom. Meanwhile, there is a weak interaction between the sulfur atom on -SCN group and a hydrogen atom of methyl group. The F–Li distance is 1.854 Å and the sulfur is 3.835 Å from the hydrogen. In another complex **3b′**, the nitrogen atom is more close to the hydrogen atom on the methyl group. The F–Li distance is 1.847 Å and the nitrogen is 2.712 Å from the hydrogen. The LiNCS moiety still keeps linear structure in **3c′**. The Li–S distance in **3a′**, and Li–N distances in **3b′** and **3c′** become longer than in reactant.

Reaction of CH_3F with LiNCS releases MP2(full) complexation enthalpies 65.8 (**3a′**), 74.7 (**3b′**) and 70.8 kJ/mol (**3c′**), respectively, which are close to 77.9 kJ/mol found in the complex $CH_3F \cdots LiF$ at the MP2(full)/6-31+G(d) level [10]. The shorter Li–F and N–H distances make **3b′** more stable than **3a′** by 8.9 kJ/mol.

The effects of $CH_3F \cdots LiNCS$ complexation are twofold: (1) it increases the C–F bond distance in the free reactants from 1.365 to about 1.41 Å in **3a′–c′**, and (2) it increases the effective positive charge on the CH_3 group in the complex $H_3CF \cdots LiNCS$ from +0.43 to about +0.50e(**3a′–c′**), respectively. Both of them are favorable for the proceeding of the subsequent nucleophilic attack.

TRANSITION STATE STRUCTURES

In this part, all of the relative energies are evaluated by the Gibbs free energies (ΔG_{298}) unless otherwise stated.

Two inversion transition structures were located for the reaction of thiocyanate anion and methyl fluoride. The TS structure, $[NCS\cdots CH_3\cdots F]^{-\neq}$ (**4a**), is 7.7 kJ/mol lower than another TS structure, $[SCN\cdots CH_3\cdots F]^{-\neq}$ (**4b**). Calculated results show a preference for sulfur in the thiocyanate anion as the attacking site in the inversion pathway, which is different from the one found in the analogous reaction of cyanate ion and methyl fluoride, where the transition structure $[NCO\cdots CH_3\cdots F]^{-\neq}$ is 27.7 kJ/mol higher than $[OCN\cdots CH_3\cdots F]^{-\neq}$ [11]. These results imply the main initial product will be methyl thiocyanate in the ionic S_N2 reaction.

Four TS structures, $[LiNCS/CH_3F]^{\neq}$(**4a′–d′**), were found for the inversion mechanism of the reaction of lithium thioisocyanate and methyl fluoride. One nucleophilic site (N) of the isothiocyanate coordinates with lithium, and the other nucleophilic site (S) attacks methyl fluoride, leading to a planar six-membered ring TS structure (**4a′**). In another planar six-membered ring TS structure **4b′**, the nucleophilic site (S) of the isothiocyanate coordinates with lithium and the other nucleophilic site (N) attacks methyl fluoride from backside of central carbon atom. If the same atom (S or N) on the LiNCS moiety coordinates with lithium and attacks methyl fluoride from backside simultaneously, forming a planar four-membered ring TS structure (**4c′** or **4d′**). In the six-membered ring TS structures, **4a** and **4b**, the bridging actions of the lithium cation cause smaller geometry changes relative to the anionic S_N2 TS structures, the S–C–F and N–C–F angles decreasing from 180° to ≈140°, which is larger than that found in the other two four-membered ring TS structures (**4c′** and **4d′**) by ≈60°. These geometric characteristics reduce the repulsion between nucleophilic site and the leaving group and stabilize the transition structures **4a′** and **4b′**.

We define the composite looseness of transition structure, $\%L^{\neq}$, in a way similar to that proposed by Shaik et al. [20]

$$\%L^{\neq} = \%\text{C-F}^{\neq} + \%\text{C-S}^{\neq}\ (\text{or}\ \%\text{C-N}^{\neq}) \tag{4}$$

$$\%\text{C-F}^{\neq} = 100[r^{\neq}(\text{C-F}) - r^{R}_{\text{com}}(\text{C-F})]/r^{R}_{\text{com}}(\text{C-F}) \tag{5}$$

$$\%\text{C-S}^{\neq} = 100[r^{\neq}(\text{C-S}) - r^{P}_{\text{com}}(\text{C-S})]/r^{P}_{\text{com}}(\text{C-S}) \tag{6}$$

$$\%\text{C-N}^{\neq} = 100[r^{\neq}(\text{C-N}) - r^{P}_{\text{com}}(\text{C-N})]/r^{P}_{\text{com}}(\text{C-N}), \tag{7}$$

where $r^{\neq}$(C–F) is the C–F bond length in the four transition structures (**4a′–d′**); $r^{\neq}$ (C–S) is the C–S bond length in TS structures **4a′** and **4c′**; $r^{\neq}$ (C–N) is the C–N bond length in TSs **4b′** and **4d′**; r^{R}_{com} (C–F) is the C–F bond length in reactants dipole–dipole complex **3a′–c′**; r^{P}_{com} (C–S) is the C–S bond length in the products dipole–dipole complex **5a′**; r^{P}_{com} (C–N) is the C–N bond length in the products dipole–dipole complex **5b′**. It was found the %L values of **4c′** (144.9) and **4d′** (116.2) are much larger than those in **4a′** (84.4) and **4b′** (99.4), respectively.

The activation barriers relative to reactants increase in the order: 120.7 (**4a′**) < 165.8 (**4b′**) < 250.6

(**4d′**) < 299.0 kJ/mol (**4c′**). Generally, the six-membered ring TS structures (**4a′** and **4b′**) are lower in energy than are the four-membered ring TS structures (**4c′** and **4d′**), because the much smaller S–C–F and N–C–F angles in **4c′–d′** increase the repulsion between the anionic nucleophilic site and leaving group. Previous studies [21] on the gas-phase nonidentity S_N2 reactions of halide anions with methyl halides pointed out that there was a reasonable correlation between the activation barriers relative to reactants complex and the looseness, $\%L^{\neq}$, the larger is the $\%L^{\neq}$ value, the higher is the barrier. So the larger S–C–F and N–C–F angles and smaller $\%L^{\neq}$ values lead to the lower reaction barriers of **4a′–b′** than **4c′–d′**. Moreover, **4a′** is lower in energy than is **4b′**, by 45.1 kJ/mol, which can be explained by the shorter Li–N distance in **4a′** and the longer S–Li distance in **4b′** than the corresponding reactants complexes, **3a′** and **3b′,** the stronger Li–N interaction makes **4a′** more stable than **4b′**.

One noteworthy feature of ion-pair reaction is that the activation barrier with respect to reactants for TS (**4a′**) is much lower than the corresponding barrier in the anionic reaction for TS (**4a**), by 37.7 kJ/mol (73.4 vs. 111.1kJ/mol in terms of ΔH_{298}), in contrast to the identity reaction of lithium fluoride and methyl fluoride [13], where the barrier for TS, $[LiF/CH_3F]^{\neq}$, is higher than $[F\cdots CH_3\cdots F]^{-\neq}$ by ≈210 kJ/mol ($\Delta\Delta H_{298}$). The remarkable phenomena may be attributed to two factors: (1) the larger S–C–F angle (≈140°) in six-membered TS structure **4a′** reduces the repulsion between $S^-\cdots\cdots F^-$; (2) the shorter Li-N and Li-F distances stabilize **4a′** and lower the reaction barrier. As for the comparison between the two four-membered ring TS structures (**4c′** and **4d′)**, the more stable LiNCS moiety than LiSCN will leads to **4d′** being lower energy.

EXPLORING REACTION PATHWAYS

It is obvious that there are two possible reaction pathways for the inversion mechanism of the reaction of thiocyanate anion and methyl fluoride (see Fig.1). One is via R-com (**3a**), TS (**4a**), and P-com (**5a**). Finally, initial product CH_3SCN (**6a**) is formed. In another pathway, the initial step is the formation of complex (**3b**), passing through the transition structure (**4b**) and the product's ion–dipole complex (**5b**) to reach another stable product CH_3NCS (**6b**). The comparable activation barrier gap ($\Delta\Delta H_{298}$ = 7.2 kJ/mol) between sulfur and nitrogen as the attacking site is less than the corresponding value (≈28 kJ/mol) in the reaction of cyanate ion and methyl fluoride [11], which implies that the two routes are competitive even though the initial product CH_3SCN is kinetic control.

For the inversion mechanism of the reaction of lithium thiocyanate and methyl fluoride, there may be four possible reaction pathways (see Fig. 2). In pathways **I** and **II**, the reaction starts with the formation of reactants dipole–dipole complex, **3a′**. The reaction progresses via different transition structure **4a′** or **4c′,** respectively. Continuing on, the sulfur atom on SCN moiety moves toward the central carbon, fluorine away from the carbon and closer to the lithium, reaching the product's dipole–dipole complex **5a′**. Finally, the product's complex will dissociate into methyl thiocyanate and lithium fluoride.

In other two pathways (**III** and **IV**), the initial step is the coordination of T-shape LiNCS (**2a′**) or linear LiNCS (**2b′**) to the fluorine atom on CH_3F to form the R-com, **3b′** or **3c′.** Reaction progresses via different TS structure **4b′** or **4d′**. Then, the nitrogen atom on NCS moiety moves toward the central carbon, fluorine away from carbon and closer to the lithium, reaching the P-com **5b′,** which subsequently dissociates into methyl isothiocyanate and lithium fluoride.

Based on analyses of energetics in Table II, methyl thiocyanate is the initial product for both the ionic [Eq. (3)] and ion pair S_N2 reactions [Eq. (2)]. A stronger preference for sulfur in the T-shape lithium thiocyanate as attacking site is observed in the ion pair S_N2 reaction. Moreover, the comparison between the ionic and ion pair S_N2 reaction shows that the introduction of lithium significantly lowers the reaction barrier, while changing the displacement reaction from endothermic to exothermic.

Conclusions

Application of MP2(full) theory to gas-phase anionic and ion-pair S_N2 reactions NCS^- + CH_3F and LiNCS + CH_3F with inversion mechanism leads to the following conclusions: (1) there are two possible reaction pathways via the different reactants ion–dipole complexes and TS structures for the reaction NCS^- + CH_3X, shown in following equations:

$$
\begin{aligned}
NCS^- + CH_3X &\rightarrow NCS^- \cdots CH_3F \\
&\rightarrow [NCS \cdots CH_3 \cdots F]^{-\neq} \rightarrow NCSCH_3 \cdots F^- \\
&\rightarrow CH_3SCN + F^-
\end{aligned}
$$

$$\begin{aligned} SCN^- + CH_3X &\rightarrow SCN^- \cdots CH_3F \\ &\rightarrow [SCN \cdots CH_3 \cdots F]^{-\neq} \rightarrow SCNCH_3 \cdots F^- \\ &\rightarrow CH_3NCS + F^-. \end{aligned}$$

According to the comparison between above two TS structures, methyl thiocyanate was predicted to be the initial product in the ionic reaction; (2) for the ion pair S_N2 reaction LiNCS + CH_3F with inversion mechanism, the following four possible reaction pathways are predicted:

$$\textbf{I}: \text{LiNCS } (\mathbf{2a'}) + CH_3F \rightarrow \text{R-com } (\mathbf{3a'}) \rightarrow \text{TS } (\mathbf{4a'}) \rightarrow \text{P-com } (\mathbf{5a'}) \rightarrow CH_3SCN\ (\mathbf{6a}) + \text{LiF}$$

$$\textbf{II}: \text{LiNCS } (\mathbf{2a'}) + CH_3F \rightarrow \text{R-com } (\mathbf{3a'}) \rightarrow \text{TS } (\mathbf{4c'}) \rightarrow \text{P-com } (\mathbf{5a'}) \rightarrow CH_3SCN\ (\mathbf{6a}) + \text{LiF}$$

$$\textbf{III}: \text{LiNCS } (\mathbf{2a'}) + CH_3F \rightarrow \text{R-com } (\mathbf{3b'}) \rightarrow \text{TS } (\mathbf{4b'}) \rightarrow \text{P-com } (\mathbf{5b'}) \rightarrow CH_3NCS\ (\mathbf{6b}) + \text{LiF}$$

$$\textbf{IV}: \text{LiNCS } (\mathbf{2b'}) + CH_3F \rightarrow \text{R-com } (\mathbf{3c'}) \rightarrow \text{TS } (\mathbf{4d'}) \rightarrow \text{P-com } (\mathbf{5b'}) \rightarrow CH_3NCS\ (\mathbf{6b}) + \text{LiF}.$$

The six-membered ring TS structure involved in the first pathway is much lower in energy than are the others, and methyl thiocyanate should form preferentially, which is in agreement with the experiments; (3) combining the MP2(full) results of kinetic and thermodynamic investigations, the introduction of lithium cation will make the ion pair reaction LiNCS + CH_3F a more facile process than the anionic reaction F^- + LiNCS; (4) methyl isothiocyanate is more stable than is methyl thiocyanate, by 4.9 kJ/mol; in terms of ΔG_{298}, the former can be prepared by thermal rearrangement of methyl thiocyanate via methyl transfer; (5) both anionic and ion-pair reaction share the same interesting feature—the thermodynamically favorable product CH_3NCS has a higher barrier. The difference in barrier is, however, smaller in the anionic reaction, with 7.7 kJ/mol compared with the value 45.1 kJ/mol [120.7 kJ/mol (**I**) versus 165.8 kJ/mol (**III**) in terms of ΔG_{298}] in the ion-pair reaction. Therefore, the ion-pair reaction is more selective, and the initial product is kinetic control and dominated by thermodynamically unfavorable CH_3SCN. It is very consistent with the experimental results.

ACKNOWLEDGMENTS

One of the authors (H.-J. Zhu) acknowledges the support of Bairenjihua Fund from CAS. One of the authors (Y. Ren) is thankful for the support from the Scientific Research Foundation for the Returned Chinese Scholars of State Education Ministry and Sichuan University. One of the authors (S.-Y. Chu) thanks NSC of Taiwan for financial support.

References

1. Patai, S. Ed. The Chemistry of Cyanates and Their Thio Derivatives; John Wiley & Sons: New York, 1977.
2. Cremlyn, R. J. An Introduction to Organosulfur Chemistry; John Wiley & Son Ltd. Chichester, 1996.
3. Winstein, S.; Savedoff, L. G.; Smith, S.; Stevens, I. D. R.; Gall, J. S. Tetrahedron Lett 1960; p 24.
4. Cayzergues, P.; Georgoulis, C.; Mathieu, G. J. Chim Phys Phys Chim Biol 1987, 84, 63.
5. Westaway, K. C.; Waszczylo, Z.; Smith, P. J.; Rangappa, K. S. Tetrahedron Lett 1985, 26, 25.
6. Westaway, K. C.; Lai, Z.-G. Can J Chem 1988, 66, 1263.
7. Westaway, K. C.; Lai, Z.-G. Can J Chem 1989, 67, 345.
8. Lai, Z.-G.; Westaway, K. C. Can J Chem 1989, 67, 21.
9. Harder, S.; Streitwieser, A.; Petty, J. T.; Schleyer, P. v. R. J Am Chem Soc 1995, 117, 3253.
10. Streitwieser, A.; Choy, G. S-C.; Abu-Hasanayn, F. J Am Chem Soc 1997,119, 5013
11. Leung, S. S.W.; Streitwieser, A. J Comput Chem 1998, 19, 1325.
12. Ren, Y.; Chu, S.-Y. Chem Phys Lett 2003, 376, 524.
13. Ren, Y.; Chu, S.- Y. J Comput Chem 2004, 25, 461.
14. Veszprémi, T.; Pasinszki, T.; Feher, M. J Am Chem Soc 1994, 116, 6303.
15. Møller, C.; Plesset, M. S. Phys Rev 1934, 46, 618.
16. Scott, A. P.; Radom, L. J Phys Chem. 1996, 100, 16502.
17. Reed, A. E.; Weinstock, R. B.; Weinhold, F. J Chem Phys 1985, 83, 735.
18. Frisch, M. J.; Trucks, G. W.; Schlegel, H. B.; Scuseria, G. E.; Robb, M. A.; Cheeseman, J. R.; Zakrzewski, V. G.; Montgomery, J. A.; Stratmann, R. E.; Burant, J. C.; Dapprich, S.; Millam, J. M.; Daniels, A. D.; Kudin, K. N.; Strain, M. C.; Farkas, O.; Tomasi, J.; Barone, V.; Cossi, M.; Cammi, R.; Mennucci, B.; Pomelli, C.; Adamo, C.; Clifford, S.; Ochterski, J.; Petersson, G. A.; Ayala, P. Y.; Cui, Q.; Morokuma, K.; Malick, D. K.; Rabuck, A. D.; Raghavachari, K.; Foresman, J. B.; Cioslowski, J.; Ortiz, J. V.; Stefanov, B. B.; Liu, G.; Liashenko, A.; Piskorz, P.; Komaromi, I.; Gomperts, R.; Martin, R. L.; Fox, D. J.; Keith, T.; Al-Laham, M. A.; Peng, C. Y.; Nanayakkara, A.; Gonzalez, C.; Challacombe, M.; Gill, P. M. W.; Johnson, B. G.;

Chen, W.; Wong, M. W.; Andres, J. L.; Head-Gordon, M.; Replogle, E. S.; Pople, J. A. Gaussian 98 (Revision A.9); Gaussian: Pittsburgh, 1998.

19. Kotani, M.; Shigetomi, Y.; Imada, M.; Ōki, M.; Nagaoka, M. Heteroatom Chem 1997, 8, 35.
20. Shaik, S. S.; Schlegel, H. B.; Wolfe, S. Theoretical Aspects of Physical Organic Chemistry: The S_N2 Mechanism; Wiley: New York, 1992.
21. Glukhovtsev, M. N.; Pross, A.; Schlegel, H. B.; Bach, R. D.; Radom, L. J Am Chem Soc 1996, 118, 11258.